Measurement of restricted and hindered anisotropic diffusion tissue compartments in a rat model of Wallerian degeneration

Benoit Scherrer[1], Damien Jacobs[2], Maxime Taquet[1,2], Anne des Rieux[3], Benoit Macq[2], Sanjay P Prabhu[1], and Simon K Warfield[1]

[1]Department of Radiology, Boston Children's Hospital, Harvard Medical School, Boston, MA, United States, [2]ICTEAM, Universite catholique de Louvain, Louvain-La-Neuve, Belgium, [3]LDRI, Université catholique de Louvain, Brussels, Belgium

Synopsis

The DIAMOND model has been recently proposed to model the heterogeneity of tissue compartments in diffusion compartment imaging. However, it did not enable the characterization of the intra-axonal volume fraction (IAVF), a critical measure to more accurately characterizing axonal loss in abnormal tissues. In this work we investigated mathematical extensions to DIAMOND that model both the IAVF and the heterogeneous nature of in-vivo tissue. We validated our approach using both Monte-Carlo simulations and histological microscopy with an animal model of Wallerian degeneration. We show that our novel model better predicts the signal and provides additional parameters to further describe tissues.

Purpose

In a recent work, Scherrer et al[1] proposed a novel diffusion compartment imaging (DCI) model that describes the statistical distribution of 3-D diffusivities arising from each compartment in each voxel (DIAMOND), allowing for the characterization of both compartment-specific diffusion parameters (cFA, cMD, cAD, cRD) and the overall compartment microstructural heterogeneity. DIAMOND was shown to better predict the DW signal compared to NODDI[2]. However, it did not enable characterization of the intra-axonal volume fraction (IAVF), a critical measure to more accurately characterizing axonal loss in abnormal tissues. In this work, we investigated mathematical extensions to DIAMOND that model both the IAVF and the heterogeneous nature of in-vivo tissue. We first used Monte-Carlo simulations to identify the best candidate model to estimate IAVF. Then, we validated our novel approach using an animal model of Wallerian degeneration and histological observations.

Method

Mathematical modeling. In the original DIAMOND formulation, the combined contribution of intra-axonal (IA) restricted and extra-axonal (EA) hindered diffusion was modeled by a single statistical distribution of diffusivities[1]. In this work, we instead considered models that separately represent IA and EA diffusion arising from a fascicle[3], by considering: $S_f = \gamma S_{IA} + (1-\gamma) S_{EA}$ (with S_f: signal arising from a fascicle; S_{IA},S_{EA}: signal arising from IA/EA space, respectively; γ: IAVF). S_{IA} was modeled using the analytic expression of the diffusion in cylinders.[3] S_{EA} was modeled using a matrix-variate Gamma distribution of diffusivities to capture the intra-compartment heterogeneity.[1] We evaluated three different estimation strategies: *1) DIAMOND+H1*: a model in which the radial diffusivities of IA/EA compartments ($d_{IA}^{\perp}$/$d_{EA}^{\perp}$) are freely estimated; *2) DIAMOND+H2*: models in which $d_{IA}^{\perp}$ is fixed and $d_{EA}^{\perp}$ is estimated; and *3) DIAMOND+H3*: a model using a simplified tortuosity model, by setting $d_{EA}^{\perp} = (1-\gamma) d_{EA}^{\parallel}$.[4, 5] In all models, the orientation of diffusion and IA/EA axial diffusivities were forced to be equal.

Monte-Carlo simulations. We simulated the signal arising from aligned cylinders of radius R=0.5µm with increasing IAVF (Camino simulator[6], 200,000 walkers, 5000 time points, gradient pulse duration and separation δ=4.5ms and Δ=12 ms). The gradient scheme included 12 non-weighted images and 6 shells of 36 gradients directions each at b-values: 300, 700, 1500, 2800, 4500, 6000s/mm². We compared the estimated IAVF to the known, ground truth values. We also compared results to those obtained with NODDI[2].

Histological validation. We performed a left-unilateral rhizotomy on 3 rats at L2-L3 levels, inducing Wallerian degeneration in the ipsilateral gracile fasciculus (GF). A laminectomy was also performed on 3 control rats (shams) at identical L2-L3 levels. For each rat, in-vivo diffusion weighted imaging (DWI) was performed at 11.7T (resolution: 0.1x0.1x1mm3) 51 days post-injury with the gradient scheme used in our Monte-Carlo simulations. After acquisition, the rats were perfused, spinal cord was removed, cryoprotected before being frozen and stored at -80°C, sliced axially in 20µm thick section using cryostat. Immunostainings were performed for myelin

(LFB), neurofilaments (SMI312), and microglia (Iba1). We semi-automatically segmented axons on SMI312 stainings, myelin on LFB stainings and vesicles on Iba1 stainings. DW images were resampled to 0.1x0.1x0.1mm^3 and corrected for animal motion and eddy-current distortion using affine registration to the b=0s/mm^2 image. We evaluated DIAMOND+H3 with, in addition, two isotropic diffusive components: one with fixed diffusivity ($D_{free} = 3.0e^{-3}$s/mm2) and one whose diffusivity D_{iso} was estimated. Model parameters were assessed in ROIs (~5000 voxels) drawn in the GF in the ipsilateral (lesion) and controlateral (healthy) parts of the spinal cords. We also compared DIAMOND+H3 to the minimal model of white matter diffusion (MMWMD)[4], which models S_{EA} with a single diffusion tensor instead of a distribution of 3-D diffusivities, by assessing their generalization error (GE)[7].

Results

Fig.1a shows that estimating both $d_{IA}^{\perp}$ and $d_{EA}^{\perp}$ does not enable robust estimation of IAVF. Fig.1b shows that a model in which the IA compartment cylinders radius R is prefixed is sensitive to the choice of R, which is unknown in-vivo. Ultimately, DIAMOND+H3 provides the more robust IAVF estimation (Fig.1c) and favorably compares to that of NODDI (Fig.1d).

Fig.2 reports the results from our rhizotomy experiment. It shows a statistically significant decrease of IAVF in the ipsilateral part (Fig.2b) which is validated using SMI312 staining. Fig.3 synthesizes other findings. Fig.4 shows a slice in which IAVF accurately correlates with our neurite ratio (Fig.2m). Finally, Fig.5 shows DIAMOND+H3 has a lower GE than MMWMD.

Conclusion

Our extension to DIAMOND enables estimation of the IAVF in vivo. We show that the prediction error is smaller when modeling EA diffusion with a statistical distribution of tensors instead of a single tensor. Compared to NODDI, our new model also provides additional compartment-specific parameters (cRD, cAD) to further describe tissues.

Acknowledgements

This work was supported in part by NIH grants R01 NS079788, R01 EB018988, U01 NS082320, Intel (c) IPCC, BCH CTREC K-to-R Merit Award and BCH TRP Pilot.

References

1. Scherrer, B., A. Schwartzman, M. Taquet, M. Sahin, S.P. Prabhu, and S.K. Warfield, Characterizing brain tissue by assessment of the distribution of anisotropic microstructural environments in diffusion-compartment imaging (DIAMOND). Magn Reson Med, 2015: p. to appear.

2. Zhang, H., T. Schneider, C.A. Wheeler-Kingshott, and D.C. Alexander, NODDI: practical in vivo neurite orientation dispersion and density imaging of the human brain. Neuroimage, 2012. 61(4): p. 1000-16.

3. Assaf, Y., R.Z. Freidlin, G.K. Rohde, and P.J. Basser, New modeling and experimental framework to characterize hindered and restricted water diffusion in brain white matter. Magn Reson Med, 2004. 52: p. 965-78.

4. Alexander, D.C., P.L. Hubbard, M.G. Hall, E.A. Moore, M. Ptito, G.J. Parker, and T.B. Dyrby, Orientationally invariant indices of axon diameter and density from diffusion MRI. Neuroimage, 2010. 52(4): p. 1374-89.

5. Szafer, A., J. Zhong, and J.C. Gore, Theoretical model for water diffusion in tissues. Magn Reson Med, 1995. 33(5): p. 697-712.

6. Hall, M.G. and D.C. Alexander, Convergence and parameter choice for Monte-Carlo simulations of diffusion MRI. IEEE Trans Med Imaging, 2009. 28: p. 1354-64.

7. Efron, B., Estimating the error rate of a prediction rule: improvement on cross-validation. Journal of the American Statistical Association, 1983. 78(382): p. 316-331.

Figures

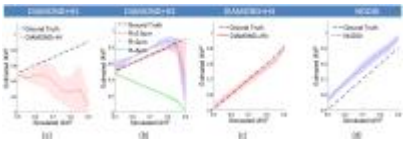

(a-c) Results from the Monte-Carlo simulations with the models DIAMOND+H1, DIAMOND+H2 (for various prefixed values of R) and DIAMOND+H3. The curves show the mean and standard deviation of the estimated IAVF over 100 independent repetitions. The best results are obtained with DIAMOND+H3 (c). This model compares favorably to NODDI (d).

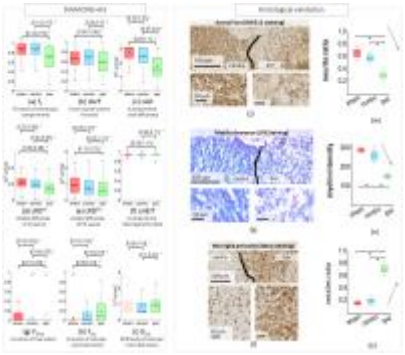

(a-i): Estimated model parameters and correlation with histology (solid circle: mean; thick horizontal line: median). Statistical significance ($p<0.001$) is indicated with * together with confidence intervals; (j-l): Histological validation with various staining; (m-o) : Quantitative evaluation based on the histology.

DCI model parameters	Interpretation	Link to histology
↘ FI	Overall, there is less anisotropic diffusion in voxels	↘ neurite ratio Axonal death (Fig.2J)
↘ IAVF	In the remaining anisotropic diffusion, the relative amount of intra-axonal water is reduced	↘ neurite ratio Axonal death (Fig.2J)
↘ IAD	The ability of water molecules to diffuse along the remaining axons is reduced	↘ myelin intensity (Fig.2J) IADs reduced because of myelin and axonal debris.
↘ $rD^{EA}_{\perp}$	The ability of water molecules to diffuse radially in the IA space is reduced	Unclear.
↘ rD^{EA}	The ability of water molecules to diffusion radially in the EA space is reduced.	↘ neurite ratio (Fig.2J) As the density of axons decreases, the probability that a water molecule bounces against an axonal membrane decreases, leading to an increase in isotropic diffusion. The water molecules bouncing on the remaining axons are much closer to these axons, leading to an overall reduced rD^{EA}.
↘ rD^{EE}	The environment composed of the remaining axons is more homogeneous.	Unclear
D_{iso} and ↗ f_{iso}	An isotropic restricted diffusion environment appears, with D_{iso}=1e-3s/mm2.	↗ vesicles ratio (Fig.2k) Microglial activation and phagocytosis lead to a substantial increase in the number of vesicles

Table synthesizing the interpretation of DCI model parameter changes together with our histological observations.

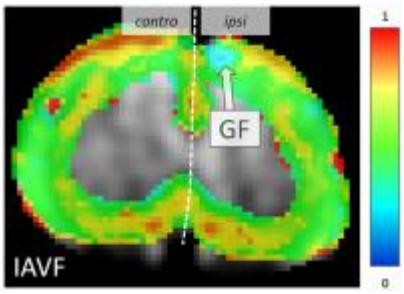

(a) Map of IAVF in the WM superposed on a b=0 image for an injured rat. In this slice, a low IAVF≈0.2 (See also Fig.2l) is estimated in the gracile fasciculus (GF) in the ipsilateral side, i.e. where Wallerian degeneration is expected. Other patterns in IAVF are mostly symmetrical.

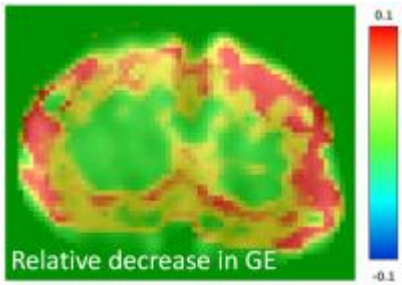

Map of the relative decrease of the generalization error between MMWMD and DIAMOND+H3. The generalization error is substantially smaller when modeling the heterogeneous nature of tissue in the WM (decrease up to 10%).

Proc. Intl. Soc. Mag. Reson. Med. 24 (2016)
1087